

On global changes in effective cloud height

Amato T. Evan¹ and Joel R. Norris¹

Received 25 July 2012; revised 28 August 2012; accepted 1 September 2012; published 6 October 2012.

[1] Measurements by the Multiangle Imaging Spectro-Radiometer (MISR) instrument exhibit a decreasing trend in global mean effective cloud top height (2000–2011). Here we show that this trend is likely related to an artifact in the data present during the early years of the MISR mission that caused a systematic reduction in the number of retrievals of clouds at lower elevations relative to clouds at higher elevations. After the application of a *post-hoc* method for removing the bias associated with missing retrievals the MISR effective cloud height anomalies exhibit a positive trend over time. **Citation:** Evan, A. T., and J. R. Norris (2012), On global changes in effective cloud height, *Geophys. Res. Lett.*, 39, L19710, doi:10.1029/2012GL053171.

1. Introduction

[2] Clouds represent a major source of uncertainty in models of the Earth’s climate response to man-made global warming. As the world warms, changes in cloud cover and cloud properties could, in principle, either counter or amplify the warming from growing concentrations of atmospheric CO₂. One way in which clouds alter the global energy budget is through the emission of longwave radiation to space, which is a function of the cloud emissivity and cloud top temperature. Assuming a constant temperature profile in the atmosphere, as cloud heights increase the amount of longwave radiation leaving the planet goes down and, assuming radiative balance at the top of the atmosphere, planetary temperatures will over time respond by increasing. Therefore, there may exist a positive or negative longwave “cloud height feedback” if global warming causes a systematic change in cloud heights, although the total cloud feedback is dependent on additional aspects of changes in cloud properties, like cloud emissivity and cloud fraction.

[3] A recent study used a relatively new set of observations of stereoscopically derived cloud top heights to suggest that a negative cloud height feedback may exist [Davies and Molloy, 2012, hereinafter DM12]. DM12 calculated a negative trend in global effective cloud height anomalies of -44 ± 22 m decade⁻¹ using data from the MISR instrument. If cloud top heights are indeed falling with time, the results of DM12 could indicate a powerful negative cloud feedback to global warming. Here we analyze the MISR dataset used by DM12 and

find that the downward trends they report are caused by sampling biases in the data set.

2. Data

[4] The MISR instrument measures shortwave radiances via nine along-track cameras with a fixed range of satellite zenith angles, and cloud heights are retrieved from radiance measurements at 650 nm based on the parallax effect [Muller *et al.*, 2002]. Here we examine the cloud height data from the MISR level 3 Component Global Cloud Product (CGCL) data set. The level 3 CGCL data are averaged to a 0.5° horizontal and monthly temporal resolution and reports the counts (number of observations of cloud heights) and average bin height, at each of the 15 vertical height bins, per month and per 0.5° horizontal area. Retrievals of cloud-free ocean surface are included in the Level 3 CGCL dataset as measurements of zero cloud height [Bull *et al.*, 2011]. We calculated monthly mean cloud heights at each 0.5° longitude (*i*) and latitude (*j*) location and for each month (*t*),

$$h_{ijt} = \frac{\sum_k c_{ijk} \bar{b}_{ijk}}{\sum_k c_{ijk}} \quad (1)$$

where h_{ijt} is the monthly mean cloud height at longitude *i* and latitude *j* at time *t*, c_{ijk} is the number of observations (counts) at MISR height bin *k*, for the same location and time, and \bar{b}_{ijk} is the mean height of those observations at height bin *k*. Since the cloud-free ocean surface is included as a “zero cloud height”, in addition to clouds retrieved at the lowest height bin (0–0.5 km), we refer to the monthly grid box average as an “effective cloud height”. At the time of writing MISR CGCL data were available for the time period of March 2000 through November 2011 (data from the first two months of 2000 is available but was deemed unusable because of the extremely low number of observations). Although these heights can be corrected for the effects of along-track winds on the stereoscopic retrieval [Davies *et al.*, 2007] we use the uncorrected data to be consistent with DM12.

[5] We also examine data from the daytime-only cloud height radiometrically retrieved from MODIS [Minnis *et al.*, 2011a, 2011b]. We multiplied MODIS cloud height by MODIS daytime cloud fraction [Ackerman *et al.*, 1998] to obtain an “effective cloud height”. This is the same as averaging the height of the cloudy area of a grid box with the zero height of the cloud-free area of a grid box and thus is a parameter similar to that provided by MISR.

[6] Statistical significance of all trends presented here is calculated in a manner consistent with Santer *et al.* [2000] and is reported as a p-value. In order to account for time

¹Scripps Institution of Oceanography, University of California, San Diego, La Jolla, California, USA.

Corresponding author: A. T. Evan, Scripps Institution of Oceanography, University of California, San Diego, 9500 Gilman Dr., La Jolla, CA 92093, USA. (aevan@ucsd.edu)

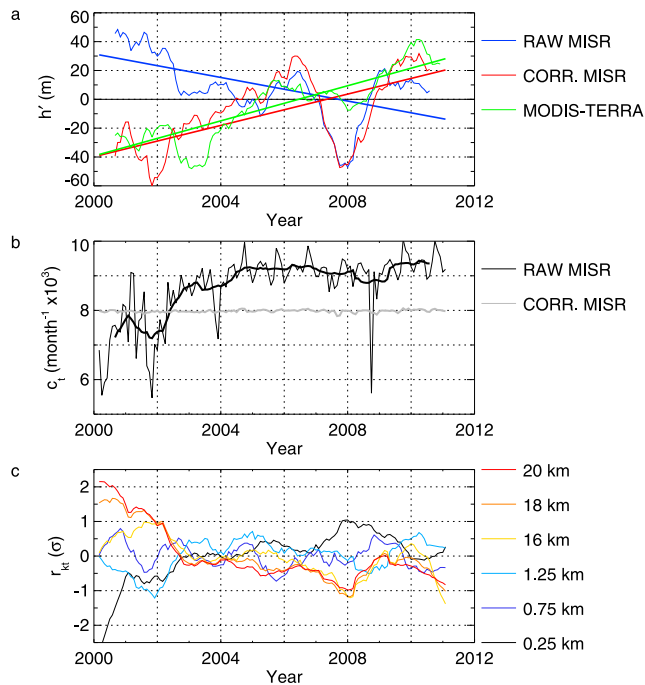


Figure 1. Time series of global mean cloud height anomalies, counts, and relative counts. (a) The smoothed (all smoothing in Figure 1 is done via a 13-month running mean filter) effective height anomaly time series (h') from MISR (blue), corrected MISR (red), and MODIS-Terra (green). Anomalies and trend lines are calculated over the period of March 2000–February 2011 using the unsmoothed data, and are indicated in Table 1. (b) Monthly mean and smoothed time series of MISR counts (black). The values on the ordinate axis represent the globally averaged number of cloud height retrievals (c_t) per $0.5^\circ \times 0.5^\circ$ grid location per month. Also shown is the monthly mean time series of the corrected MISR counts (gray). (c) The smoothed monthly mean relative counts at each MISR bin (r_{kt}), normalized by the standard deviation of each r_{kt} time series. Here the bin midpoints of the lowest and highest three MISR bins are indicated in the legend. Note that the r_{kt} anomalies are referenced to the time period of 2005–2011 in order to highlight the discrepancies at the beginning of the record. Normalization to units of standard deviation is performed to facilitate comparison of r_{kt} between the bins in the upper and lower troposphere.

series autocorrelation we use effective sample size for calculation of the adjusted standard error and the determination of the critical t -value for significance.

3. Results

[7] We calculate global MISR effective cloud height anomalies via removing from each calendar month the mean of all occurrences of that calendar month within the time series at each horizontal location. The global mean time series of effective cloud height is calculated via weighting the height fields by the cosine of latitude. The resulting global time series of effective height anomalies is very similar to that in DM12, with positive anomalies in the early part of the record, negative anomalies in the latter part of the record, and negative height anomalies during 2008 (Figure 1a). For the

period of March 2000–February 2010 the linear trend in the monthly mean unsmoothed height anomaly is $-51 \text{ m decade}^{-1}$ (p -value = 0.005), consistent with DM12.

3.1. Influence of Sampling Variations

[8] To elucidate the source of variability in the height anomaly time series (Figure 1a) we examine the MISR counts data. We calculate the global monthly mean time series of mean MISR counts, c_t , via weighting by the cosine of latitude,

$$c_t = \frac{\sum_{ijk} c_{ijk} \cos(\phi_j)}{\sum_{ijk} \cos(\phi_j)}$$

where ϕ_j is the latitude at location ijk . The time series of c_t (Figure 1b) is dominated by an increase in retrievals from the beginning of the record until late 2004, exhibiting less variance post-2005 neglecting a large drop in the number of observations that occurred in mid 2008. The variability in c_t , and in particular the upward trend in the beginning of the time series, is not physical and results from satellite orbit inclination maneuvers that rendered height retrievals inoperable due to the resultant erroneous co-registration of the nine MISR cameras (C. Moroney, personal communication, 2012; see auxiliary material).¹ These MISR camera co-registration issues were more pervasive at the beginning of the mission, resulting in the upward trend in c_t over the first five years of data.

[9] We hypothesize that this sampling problem does not affect c_t at each MISR height bin equally and is the source of the trend in the mean height anomaly time series in Figure 1a. We investigate this possibility by first creating a time series and then calculating the linear trends in globally averaged monthly mean counts at each MISR height bin, c_{kt} . The linear trends in c_{kt} are largest in the lower troposphere and diminish with height (Figure 2a), with a maximum trend of 55 counts $\text{month}^{-1} \text{ yr}^{-1}$ at the lowest (altitude) bin, and a near-zero trend at the highest bins.

[10] The downward trend in the global mean time series of MISR effective height anomalies (Figure 1a) results from the vertical gradient in the trends of c_{kt} (Figure 2a). Briefly, over time a progressively larger number of observations are being added to the lower bins than are added to the upper bins; when the variation in average height with time is calculated (equation (1)) the lower troposphere is consequently more heavily weighted, producing a downward trend in mean height anomalies (Figure 1a). A detailed discussion of how trends in c_{kt} (Figure 2a) affect the global mean height anomaly time series can be found in the Supplemental text.

[11] Variability in the time series of c_{kt} at each of the height bins is similar to that of c_t (Figure 1b), as demonstrated by the high positive correlation coefficients of c_{kt} and c_t at each height bin (Figure 2b). This suggests that variability produced by the MISR camera co-registration problem is a pervasive feature of the counts time series at every vertical level in the MISR data. In all but the highest three bins, the correlation of c_{kt} and c_t is greater than 0.85, and the highest correlations are at the three lowest height bins. The decrease

¹Auxiliary material data sets are available at <ftp://ftp.agu.org/apend/gl/2012gl053171>. Other auxiliary materials are in the HTML. doi:10.1029/2012GL053171.

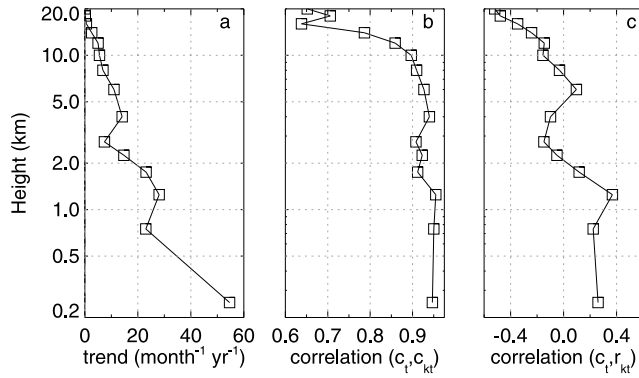


Figure 2. Characteristics of the MISR counts as a function of height. (a) The linear trends in global mean MISR counts per MISR height bin, c_{kt} , where the ordinate (for all plots) is the midpoints of the bins for which the heights are reported. Also shown are the coefficients (b) from the correlation of the global mean MISR counts, c_t (Figure 1b), and the global mean counts time series at each height bin, c_{kt} and (c) from the correlation of c_t and the relative counts at each height, r_{kt} . Trends and correlations are calculated from unsmoothed data over the time period of March 2000–February 2011.

of correlation with height suggests that the bias projects most strongly onto the counts data in the lower troposphere (we note that the sample size for each correlation coefficient is identical in Figure 2a).

[12] Further evidence that this artifact has caused the observed trends in cloud height anomalies (Figure 1a) is provided by the correlation coefficients between the time series of c_t and relative counts at each MISR bin, referred to as r_{kt} , where

$$r_{kt} = \frac{\sum_{ij} \left(\frac{c_{ijkt}}{\sum_k c_{ijkt}} \cos(\phi_j) \right)}{\sum_{ijk} \cos(\phi_j)}$$

The correlation of r_{kt} and c_t decreases with height (Figure 2c), being positive in the lower troposphere and negative in the upper troposphere. The relative counts are closely related to cloud height since they provide the weights used to calculate the mean cloud height at any location (equation (1)). Furthermore, the time series of r_{kt} for the lower troposphere exhibits a similar temporal structure to c_t , with an increase in value over the first five years of the record followed by smaller and less coherent variations, and the time series of r_{kt} for the upper troposphere is nearly identical but of inverse sign, with a decrease in value over the first five years of the record followed by less coherent variations (Figure 1c). Thus, the time series of r_{kt} also suggests that retrievals in the lower troposphere are more sensitive to the MISR camera co-registration problems than are retrievals in the upper troposphere.

3.2. Post-hoc Correction Method

[13] We attempt to quantify the influence of the sampling changes on the trends in MISR effective cloud height anomalies (Figure 1a) by applying a linear *post-hoc* method to remove the influence of the sampling issues on the height

data. At every 0.5° horizontal location, and at every MISR height bin, we remove variability in the monthly mean time series of counts at each MISR height bin that is correlated with the global total counts time series in Figure 1b via linear regression. We then reconstruct the global height anomaly time series using this “corrected” counts data and the mean bin heights as reported within the CGCL data. We note that the time series of “corrected” counts shows no variability obviously related to the MISR camera co-registration artifact (Figure 1b).

[14] The corrected global mean MISR effective height anomaly time series exhibits interannual variability that is similar to that of the uncorrected data (Figure 1a), but there is a large discrepancy at the beginning of the time series; here the uncorrected data show a decline in height while the corrected data show an increase in height of similar magnitude (Figure 1b), further evidence that the change in sampling causes the downward trends in the MISR height anomalies. Also plotted in Figure 1a is the time series of global mean effective cloud height from MODIS-Terra. For the time period of March 2000–February 2011 the MODIS-Terra and “corrected” MISR data have a statistically significant upward trend, in contrast to the statistically significant downward trend in the uncorrected MISR data (Table 1). We caution that although variability in the MODIS time series of effective cloud height is consistent with our “corrected” MISR time series, the MODIS data may also suffer from biases and thus at this point we do not consider this time series of effective cloud height to be a gold standard against which the MISR data can be evaluated. That being said, the dissimilarity between the MODIS and the “uncorrected” MISR time series of effective cloud height casts additional doubt on the physics of the trends reported in DM12.

4. Conclusions

[15] Here we reexamined MISR effective cloud height anomalies, finding that the downward trend in cloud heights reported by DM12 likely results from sampling biases in the satellite data. A linear *post-hoc* correction method to account for this bias in the heights produced a global height anomaly time series that is in closer agreement with independent datasets of effective cloud height (Figure 1a).

[16] Based on our analysis of the MISR CGCL data and the time series of the “corrected” global mean effective height anomalies, and comparisons to independent data, we conclude that it is very likely that the reduction in sampling due to the MISR camera co-registration problems result in an unphysical downward trends in the global mean time series of monthly mean MISR effective cloud height anomalies. We note that there is no obvious reason why the camera co-registration issues should affect cloud height retrievals at one height in the atmosphere more or less strongly than retrievals at another height in the atmosphere.

Table 1. Effective Cloud Height Trends^a

| | MISR | Corrected MISR | MODIS Terra |
|---------------------------------|-------|----------------|-------------|
| Trend (m decade ⁻¹) | -40.1 | +54.3 | +60.9 |

^aShown are the trends in effective cloud height from the satellite datasets based on the unsmoothed data for the time period of March 2000–February 2011. All trends are statistically significant at p-value < 0.01.

[17] It is plausible that some physical variability in the MISR counts is correlated with the sampling artifact. However, if this is the case we argue that it is impossible to separate the physical and artificial signals in the MISR height data, and that the uncertainty in the trends would be as large as the trend discrepancies between the corrected and uncorrected time data (Figure 1a). As such, our analysis does not support the conclusion from DM12 that there is a physical downward trend in MISR height anomalies.

[18] Ultimately the MISR CGCL data will be more valuable for climate studies once a solution to the camera co-registration problem is developed and the data reprocessed accordingly. DM12 suggested that the downward trends in MISR effective cloud heights could indicate a negative cloud feedback. Our analysis suggests the opposite; once inhomogeneities are accounted for there is evidence of a positive trend in MISR effective cloud height data. However, the short time period for which MISR data are available is not sufficient to provide evidence for a positive or a negative cloud height feedback associated with linear trends in the data. Furthermore, a systematic change in effective cloud height, upward or downward, need not translate to a positive or negative cloud feedback, since the feedback is dependent on a myriad of cloud properties and how they are all changing together.

[19] **Acknowledgments.** Funding for this work was provided by grants from the NOAA Climate Program Office, NA10OAR4310140 and NA10OAR4310141. We thank Andrew Dessler and Steven Sherwood for input on this work. MISR data was downloaded from the Atmospheric Science Data Center at NASA Langley Research Center, <http://eosweb>.

larc.nasa.gov. MODIS cloud height and cloud fraction data were downloaded from the NASA Langley Research Center (<http://www.larc.nasa.gov>).

[20] The Editor thanks two anonymous reviewers for assisting in the evaluation of this paper.

References

- Ackerman, S. A., et al. (1998), Discriminating clear-sky from clouds with MODIS, *J. Geophys. Res.*, *103*, 32,141–32,157, doi:10.1029/1998JD200032.
- Bull, M., J. Matthews, D. McDonald, A. Menzies, C. Moroney, K. Mueller, S. Paradise, and M. Smyth (2011), Multi-angle Imaging SpectroRadiometer (MISR) Data products specifications, *JPL Tech. Doc. D-13963*, Jet Propul. Lab., Calif. Inst. of Technol., Pasadena.
- Davies, R., Á. Horváth, C. Moroney, B. Zhang, and Y. Zhu, (2007), Cloud motion vectors from MISR using sub-pixel enhancements, *Remote Sens. Environ.*, *107*, 194–199, doi:10.1016/j.rse.2006.09.023.
- Davies, R., and M. Molloy (2012), Global cloud height fluctuations measured by MISR on Terra from 2000 to 2010, *Geophys. Res. Lett.*, *39*, L03701, doi:10.1029/2011GL050506.
- Minnis, P., et al. (2011a), CERES Edition-2 cloud property retrievals using TRMM VIRS and Terra and Aqua MODIS data, Part I: Algorithms, *IEEE Trans. Geosci. Remote Sens.*, *49*(11), 4374–4400, doi:10.1109/TGRS.2011.2144601.
- Minnis, P., et al. (2011b), CERES Edition-2 cloud property retrievals using TRMM VIRS and Terra and Aqua MODIS data, Part II: Examples of average results and comparisons with other data, *IEEE Trans. Geosci. Remote Sens.*, *49*(11), 4401–4430, doi:10.1109/TGRS.2011.2144602.
- Muller, J.-P., A. Mandanayake, C. Moroney, R. Davies, D. J. Diner, and S. Paradise, (2002), MISR stereoscopic image matchers: Techniques and results, *IEEE Trans. Geosci. Remote Sens.*, *40*, 1547–1559, doi:10.1109/TGRS.2002.801160.
- Santer, B. D., T. M. L. Wigley, J. S. Boyle, D. J. Gaffen, J. J. Hnilo, D. Nychka, D. E. Parker, and K. E. Taylor (2000), Statistical significance of trends and trend differences in layer-average atmospheric temperature time series, *J. Geophys. Res.*, *105*, 7337–7356, doi:10.1029/1999JD901105.